Energy Storage and Dissipation Notes

Note 11

July 4, 1994

DEVELOPMENT AND CHARACTERIZATION OF HIGH-FREQUENCY CAPACITORS

A. W. Kälin and B. R. Brändli
Defence Technology and Procurement Agency
NEMP-Laboratory, AC-Zentrum, CH-3700 Spiez, Switzerland

and

D. V. Giri, Pro-Tech, 3708 Mt. Diablo Boulevard, Suite 215,
Lafayette, CA 94549 USA

Abstract

The objective of this note is to perform an electrical characterization of the existing peaking capacitor arms in the Swiss MEMPS (*M*obile *EMP* *S*imulator) facility and eventually to develop improved peaking capacitors. The improvement we seek is in the frequency performance of these capacitors, while preserving other performance criteria such as high voltage and capacitance value. The improved designs are the dihedral capacitors, which have been analysed in the past. In this, note, we describe the experimental techniques useful in evaluating the frequency performance of such capacitors for high-voltage applications. The experimental results for existing as well as the new dihedral capacitors are reported. We have concluded that the dihedral capacitors offer superior high-frequency performance. Additional developmental work is required for commercial manufacturing of the new dihedral capacitors intended for high-voltage applications.

Foreword

The authors are thankful to Dr. Carl E. Baum of Phillips Laboratory, Kirtland AFB, NM, for valuable discussions during the course of this work. We are also grateful to Swiss DTPA for providing the facilities and support.

Contents

1. Introduction

Nuclear Electromagnetic Pulse (NEMP) simulators are typically energized by transient pulse generators where the stored energy in high-voltage capacitors is switched out using a spark gap. In addition, quite often, a peaking circuit is introduced between the primary storage i.e., Marx capacitor and the output switch for optimal pulser performance [1,2]. The output switch is then a key element in determining how fast the transient energy is transferred to the load. In other words, the risetime of the pulse is limited by the inductance of the switch and the pulser-load interconnection. When the pulser itself is in a biconical configuration, the peaking capacitor has dual roles of pulse shaping and wave transport. In other words, the peaking capacitor should behave like a perfect conductor at high frequencies ($\omega C >> 1$). However, owing to the nature of their construction, the peaking capacitors display both short- and open-circuit resonances. While short-circuit resonances are acceptable at high frequencies, the first open-circuit resonance poses a problem in the peaker performance. The goal of this work is to determine the frequency performance of the presently used peaking capacitors and describe experimental results for improved designs consisting of dihedral capacitors as described in [3].

2. Brief Review of Problems with Capacitors in Use

The present design is schematically shown in figure 1. It consists of two metallic foils separated by a single or multiple layers of dielectric strips, which forms an elemental capacitor (figure 1a). These elemental capacitors are typically required to operate up to 10kV and at high frequencies (100's of MHz). The elemental capacitors are wound (figure 1b) after metallic tabs are inserted and, then stacked to form a unit capacitor (figure 1c). Many stacks interconnected in series then forms a single peaking capacitor arm.

It has been observed from measurements that open-circuit resonances exist in the capacitor which limits the useful frequency range of operation. The series resonances, where the capacitor becomes a short circuit, do not present any problem, but the open circuit resonances (typically occurring at 10's of MHz) limit their use. The losses also increase as more and more elemental capacitors are series connected. Giri and Baum [3] have modeled the present peaking capacitance design with transmission lines leading to an estimation of these inherent resonances. The reactance of the capacitor was derived to be [3]

$$\tilde{Z}_{in} = \frac{1}{j\omega C}(kl)\cot(kl) \qquad (1)$$

and the first undesirable resonance occurs when the argument of the cotangent becomes π and the frequency is given by

$$f_r = \frac{c}{2l\sqrt{\varepsilon_r}} \qquad \textbf{(2)}$$

where c is the speed of light in air, l is the length of the foil in an elemental capacitor and ε_r is the relative dielectric constant of the layered dielectric between the foils.

The performance problems, especially the undesirable resonances can lead to more serious problems in the intended applications of such capacitors [4]. The new design overcomes the frequency limitation by using physically smaller elemental capacitors and connecting them in parallel to form an unit dihedral capacitor. Unit dihedral capacitors are then series connected to fabricate a peaking capacitor arm.

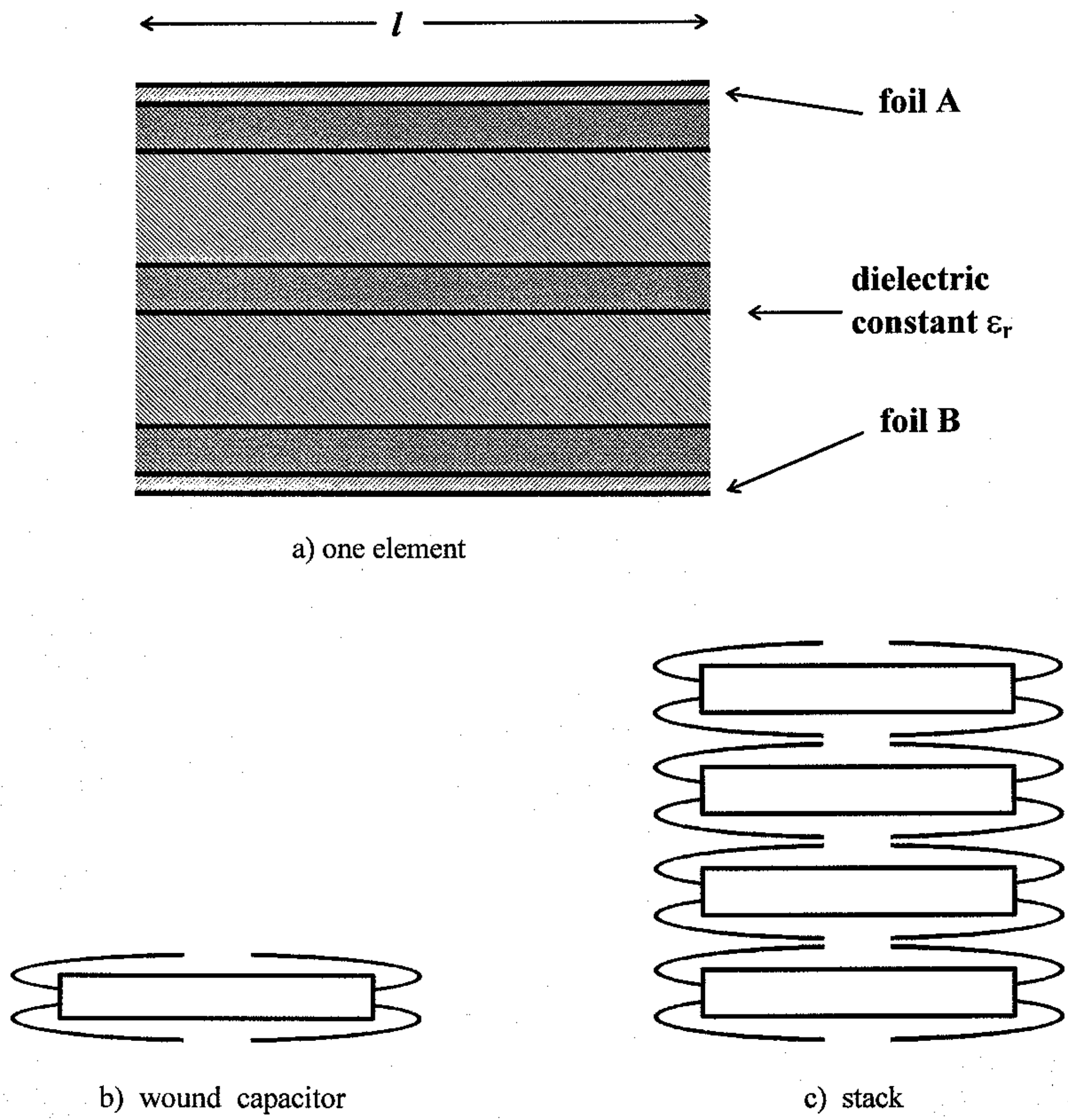

Figure 1. Existing peaking capacitor in MEMPS

3. Description of Dihedral Capacitors

Dihedral capacitors are based on the concept of introducing symmetries [3,5] in the capacitor construction. Symmetries in construction make it possible to think of the system response (e.g., capacitor current or charge) in terms of sub-groups that are mutually exclusive or non-interacting. This then makes it feasible to selectively eliminate one or the other set of resonances, resulting in improved high-frequency performance of such capacitors.

We now consider two examples of dihedral capacitors, namely $D_{1,a}$ and $D_{2,d}$, as shown in figure 2. In the illustration of $D_{1,a}$ example , there are $N_A = 3 = N_B$, or 3 each of A and B foils. In the notation of symmetry groups [5], $D_{1,a}$ is the same as $C_{2,t}$ and includes 4 elements in the group. A listing of these elements and a description of the elements may be found in [3]. Similarly we consider $D_{2,d}$ capacitor in figure 2, consisting of an equal number of A and B type of foils. This group has 8 elements listed and described in [3]. One may also note that as the subscript N of a D_N capacitor is increased, in the limit of N tending to infinity, the D_∞ capacitor becomes a parallel array of circular disc capacitors, which has been analyzed as a radial transmission line in [3].

An important distinction can be made between the $D_{1,a}$ and $D_{2,d}$ capacitors in terms of how stacking is done. A unit $D_{1,a}$ is formed as indicated in figure 2a, except that $N_A = N_B$ is some large number. Several such units are then series connected to form a single peaking capacitor arm, so that the principal axis of all the units are parallel. We observe that in $D_{1,a}$ of figure 2a all three axes, (i.e. x,y or z), are potential stack axes. In figure 2b we show the axis as stacking axis for $D_{1,a}$. The stacking axis for $D_{2,d}$ is the z-axis. $D_{1,a}$ axis (y axis) of a pad is not the same as the stacking axis (x axis). While $D_{2,d}$ units are also connected in series, the principal axes of all units are collinear. As we see later from our experimental results, the stacking of unit capacitors can also be optimized. The $D_{1,a}$ capacitor , although is of a lower order symmetry than a $D_{2,d}$ capacitor, may offer some advantage in terms of frequency performance, perhaps because of improved stacking geometry.

We have fabricated both these types of dihedral capacitors ($D_{1,a}$ and $D_{2,d}$) for experimentation. Copper foils have been used in both cases and mylar sheets as dielectrics. The dimensions of both the foils and the dielectric thickness for $D_{1,a}$ and $D_{2,d}$ were different which makes the elemental and stacked capacitances different for the two types of capacitors. Unfortunately, a direct comparison of their frequency performance is also difficult for the same reasons.

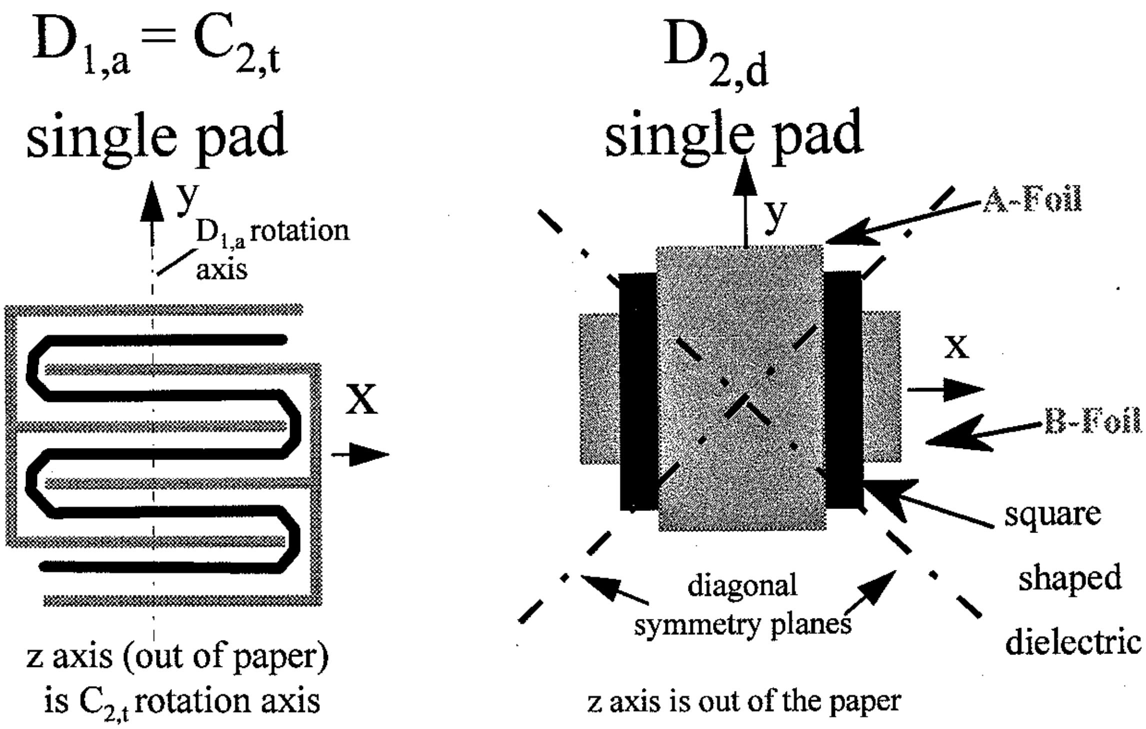

a) Two types of dihedral capacitor pads

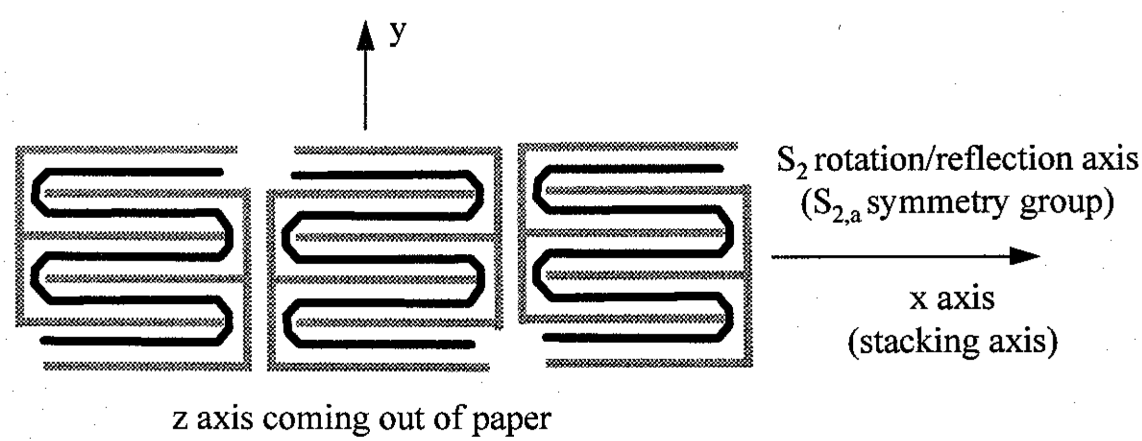

b) One Example of stacking the $D_{1,a}$ capacitor pads

Figure 2. Two Types of Dihedral Capacitors

The geometrical and electrical parameters of the two types of capacitors are listed below:

Table 1. Parameters of $D_{1,a}$ and $D_{2,d}$ Capacitors

Quantity	$D_{1,a}$ Capacitor	$D_{2,d}$ Capacitor
Copper foil dimensions	51 x 45 x 0.1 mm^3	60 x 60 x 0.05 mm^3
effective diameter	48 mm	60 mm
effective radius	24 mm	30 mm
Number of copper foils	82 per pad	approx. 48 per pad
Dielectric thickness	0.8 mm Mylar	0.23 mm Mylar
Elemental Capacitance	58.5 pF	approx. 400 pF
Capacitance of single pad	4.8 nF	19.2 nF
Capacitance of the stack	1.6 nF	2.4 nF
No. of pads/ stack	3	8

We observe from the above table that the two capacitors are not directly comparable at low or high frequencies, since their capacitance value and foil dimensions are different. $D_{1,a}$ can be expected to perform better at higher frequencies, since its foil dimensions are smaller (20 % smaller in effective radius). This concludes our description of the two capacitors and we proceed to describe the experimental setup.

4. Experimental Procedure for Evaluating Frequency Performance and Results

The frequency response of the existing peaking capacitance in MEMPS as well as the $D_{1,a}$ and $D_{2,d}$ capacitors are evaluated using the experimental setup shown in figure 3 [6]. It consists of a rectangular coaxial transmission line, whose inner conductor can be a rectangular metallic pipe. We built two versions of the rectangular transmission line shown in figure 3. The only difference between the two was the length of the central parallel section. The two lengths were respectively 1.57 m or 19 cm. The longer line could contain the entire peaking capacitor arm as an inner conductor, while the shorter line was built to accommodate single stacks of MEMPS peaker or $D_{1,a}$ or $D_{2,d}$. In addition to this coaxial rectangular transmission line, we also built an approximately 50Ω, 2-wire line by placing a conductor of rectangular cross section over a ground plane. The open 2-wire transmission line was not accurate above ≈ 200 MHz when the height of the conductor becomes (1/20) the of a wavelength. At this frequency, the separation between the two wires becomes about a tenth of a wavelength, and it no longer behaves like a simple transmission line. Since our interest is to develop capacitors performing well above 200 MHz, we concluded that the coaxial geometries are superior. We have made measurements with the following capacitors.

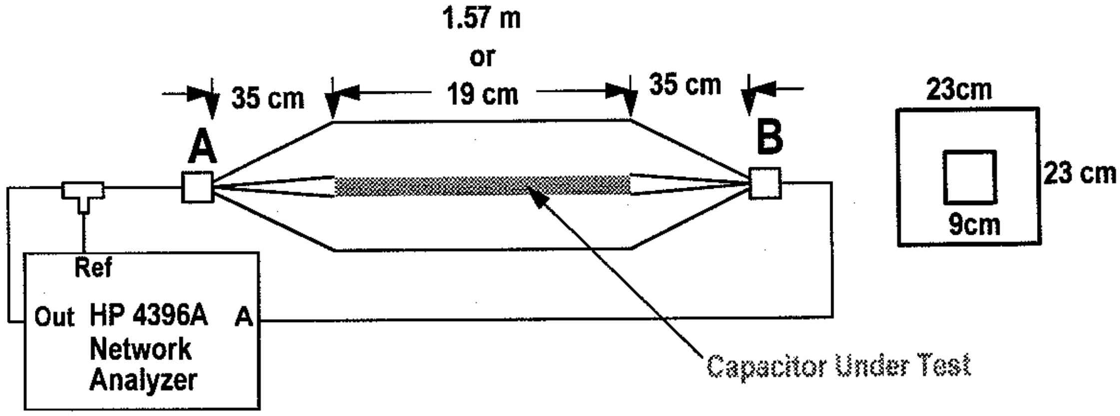

Figure 3. Experimental setup for Evaluating the Frequency Response of the Peaking Capacitors

a) a complete peaking capacitor arm from MEMPS

b) a single stack of peaking capacitor from MEMPS

c) $D_{1,a}$ stack described in Table 1

d) $D_{2,d}$ stack described in Table 1

A TDR measurement was initially performed on the peaker line to ensure that the transitions at the two ends are reasonably close to 50 Ohms and that there are no other significant discontinuities along the line. The experimental results with capacitors (a) and (b) above are shown in figure 4 and the results of dihedral capacitors are shown in figure 5.

In each of the experimental curves for the various capacitors, we also have the result for a conductive replacement for the entire inner conductor, as a reference or a base-line. The quantity plotted in figures 4 and 5, as a function of frequency is the ratio of the magnitude of the output to input voltage in dB scale. The base-line measurement also deviates from the ideal 0dB line for reasons of minor impedance discontinuities, and perhaps excitation of non-TEM modes in the air-filled coaxial line. It can also be shown that if the central region has an impedance different from the two end sections, this can lead to periodic peaks and valleys in the base-line measurement. For the present, we are looking for the first open-circuit resonance of various capacitors, and deficiencies in the measurement setup are not of big concern. We can draw the following conclusions from the experimental results.

(1) The MEMPS capacitor stack has its first undesirable resonance at 57 MHz. This is a high-Q resonance with about 18 dB loss of signal at this frequency, and highlights the frequency limitation of MEMPS peaker. There is also a deep notch at about 250 MHz (see top portion of figure 4).

(2) The above notches at 57 MHz and 250 MHz are also seen in the measurement with a single stack of MEMPS peaking capacitance (see bottom portion of figure 4).

(3) In the $D_{1,a}$ capacitor, the first open-circuit resonance of significance (more than 4 dB) occurs at a frequency well above 1 GHz, indicating an improved high-frequency performance (see top portion of figure 5).

(4) In the $D_{2,d}$ capacitor, the first open-circuit resonance of significance (more than 4 dB) occurs at a frequency of about 800 MHz, indicating an improved high-frequency performance (see bottom portion of figure 5). The resonances around 90 MHz and its harmonics are clearly due to improper impedance matching in the square rectangular transmission line. Since the cross section of the $D_{2,d}$ capacitor along the transmission line is changing with each pad, the mismatch gets enhanced.

Our measurements clearly demonstrate the superior high-frequency performance of both dihedral capacitors that we have fabricated. Since the first open-circuit resonance has been shifted-up in dihedral capacitors, deficiencies in the measurement setup become more visible. In other words, smaller problems show up when larger ones are resolved, pointing out additional developmental work.

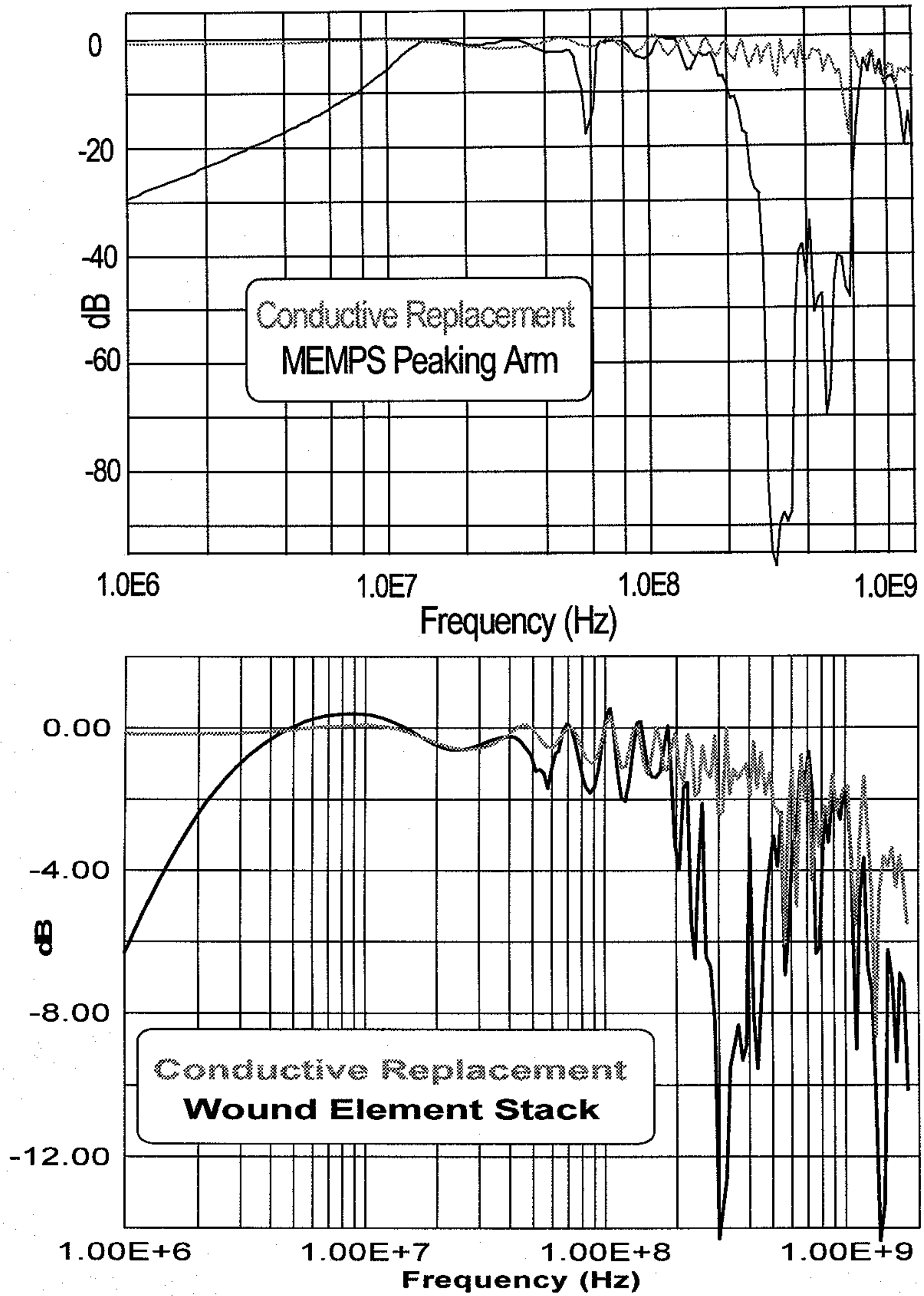

Figure 4. MEMPS Peaking Capacitor Performance

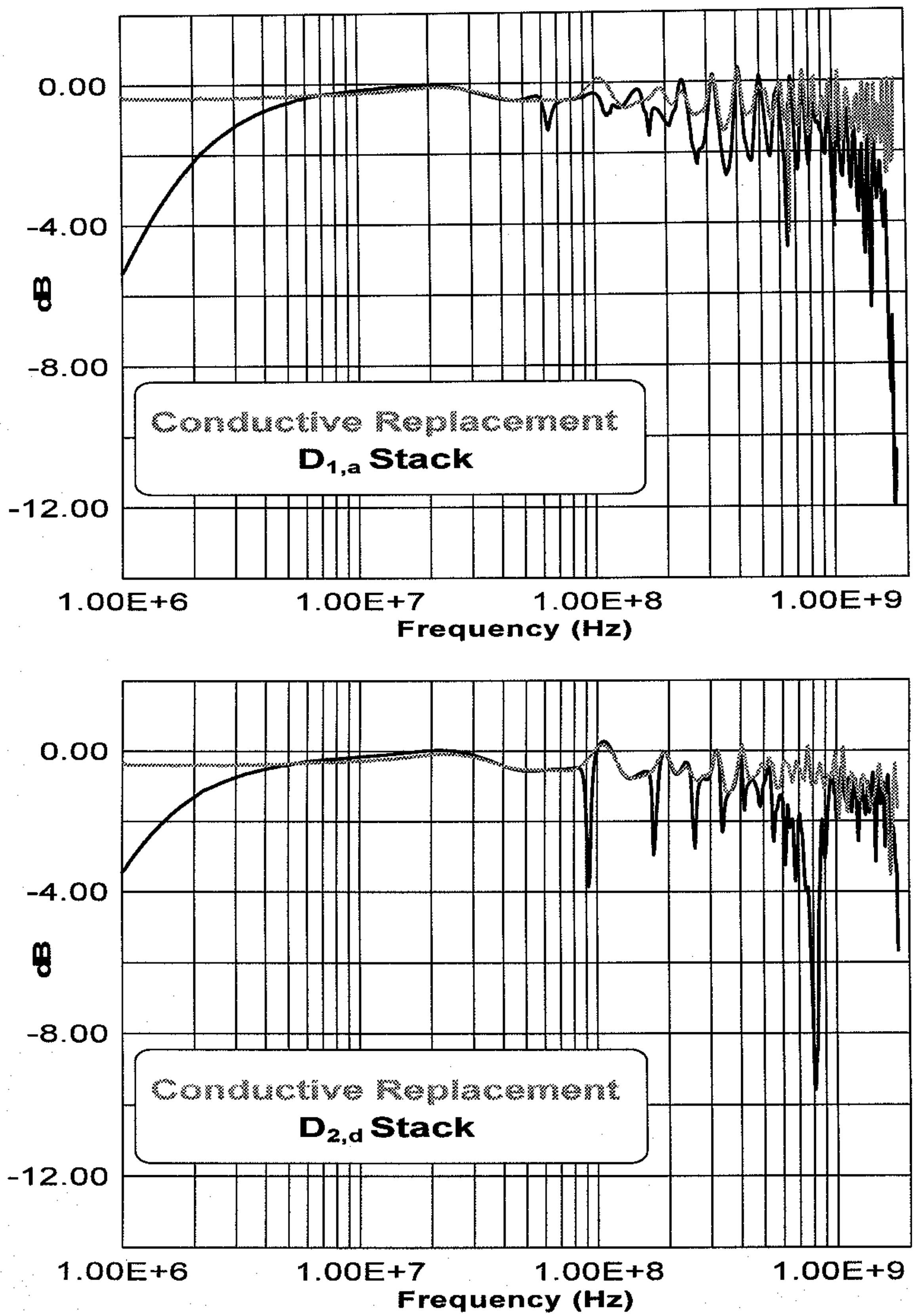

Figure 5. Dihedral Capacitor Performance

5. Dihedral Capacitors for High-Voltage Applications

$D_{1,a}$ capacitors appear to offer some advantages over the $D_{2,d}$ dihedral capacitors. In $D_{2,d}$ the $D_{2,d}$ axis of each pad is the same as stacking axis. However, in $D_{1,a}$ this is not necessarily the case. All three axes of a $D_{1,a}$ pad are potentially useful as stacking axes. We chose the stacking axis to be at right angles to the $D_{1,a}$ axis of each pad, which can help in the current flow from pad to pad. The stacking of unit capacitors seems to be more optimal in the case $D_{1,a}$ than $D_{2,d}$ capacitors. It may also be noted that industrial production of $D_{1,a}$ dihedral capacitors may be easier than the $D_{2,d}$. More importantly, the high-voltage considerations of a $D_{1,a}$ more closely resemble that of the existing peaking capacitors.

Any replacement of the existing peaking capacitor arms in MEMPS must meet the performance requirements in terms of a) higher frequencies, b) high voltage requirement , c) proper capacitance value in the available volume of space. Now that the new dihedral capacitors are validated for their high-frequency performance, the other criteria such as the capacitance value in the given volume and high-voltage considerations are to be addressed in future work.

References

1. C. E. Baum, *EMP Simulators for Various Types of Nuclear EMP Environments: An Interim Categorization*, Sensor and Simulation Note 240 , January 1978 and Joint Special Issue on the Nuclear Electromagnetic Pulse, IEEE Transactions on Antennas and Propagation, Volume AP-26, No.1, January 1978, pp. 35-53, and IEEE Transactions on Electromagnetic Compatibility, Volume EMC-20, No.1, February 1978, pp. 35-53.

2. I. D. Smith and H. Aslin, *Pulsed Power for EMP Simulators*, Joint Special Issue on Nuclear Electromagnetic Pulse, IEEE Transactions on Antennas and Propagation, Volume AP-26, No.1, January 1978, pp 53-59, and IEEE Transactions on Electromagnetic Compatibility, Volume EMC-20, No.1, February 1978, pp. 53-59.

3. D. V. Giri and C. E. Baum, *High-Frequency Capacitors*, Energy Storage and Dissipation Note 10, March 15, 1990.

4. D. V. Giri and C. E. Baum, *Theoretical Considerations for Optimal Positioning of Peaking Capacitor Arms about a Marx Generator Parallel to a Ground Plane*, Circuit and Electromagnetic System Design Note 33, 26 June 1985.

5. M. Hammermesh, *Group Theory and Its Application to Physical Problems*, Chapters 1 and 2, Addison-Wesley, Reading, MA 1962.

6. R. W. Latham, *Corrections to the Transmission-Line Parameters of a Coaxial Line when the Center Conductor has an Impedance*, Sensor and Simulation Note 168, March 1973.